Configurational Thermodynamic Properties of Polymer Liquids and Glasses. I. Poly(vinyl acetate)

John E. McKinney*[1a] and Robert Simha[1b]

Institute for Materials Research, National Bureau of Standards, Washington, D.C. 20234, and the Department of Macromolecular Science, Case Western Reserve University, Cleveland, Ohio 44106.
Received June 19, 1974

ABSTRACT: Recent experimental PVT data on poly(vinyl acetate) are analyzed using the hole theory of Simha–Somcynsky. The data were obtained at temperatures from −30 to 100° and pressures up to 800 bars. These ranges encompass the glass transition and include large portions of the liquid and glassy regions. Three different thermodynamic histories of glass formation, all isobaric cooling at 5°C/hr, were applied. With the variable formation history the glass was formed by isobaric cooling runs at different pressures. In the two constant formation histories each of the glasses was formed by a different formation pressure, namely atmospheric and 800 bars, with subsequent temperature and pressure changes in the glass in each case. In the equilibrium state good agreement between the theoretical and experimental PVT surfaces results, in accord with earlier observations on amorphous systems. As for the transitions the theory gives the correct values of dT/dP using the assumption that the hole fraction h be constant along either of the two constant formation transition lines. Similarly, the generalization of the Ehrenfest type relation involving the single ordering parameter h results in good numerical agreement with the experimental values of dT/dP for the variable formation transition line. As previously demonstrated, h does not freeze at temperatures below the glass transition, thus a constant h does not describe the structure of the glass. Parameters which describe the extent of freezing are evaluated. The fact that these parameters are independent of formation pressure would be consistent with the existence of a single entropy surface with formation pressure, as suggested by other experimental evidence.

In recent years Simha and his colleagues have investigated theoretically[2] and experimentally the equation of state and derived configurational functions for polymer liquids and glasses at atmospheric[3,4] and elevated[5] pressure. The agreement between experiment and theory for the equilibrium liquid was examined in detail. Moreover, the transition and the relationship between the liquid and the glassy states were analyzed. The formulation of the liquid state theory is particularly adapted for the latter purpose since it operates with a characteristic ordering parameter, namely the hole fraction h. Its dependence on the variables of state in each of the two states becomes then a matter of importance and serves to define quantitatively differences between liquid and glass.

Very recently McKinney and Goldstein[6] have undertaken pressure–volume–temperature (PVT) measurements of poly(vinyl acetate) in the liquid and glassy states. From the point of view summarized in the preceding paragraph these studies are especially pertinent for two reasons. First, equilibrium data are presented over ranges of temperature and pressure which are adequate to once more confront experiment and theory, although the pressure range is smaller than in the other investigations cited. Moreover, we are dealing here with the case of a glass transition at room temperature. Much of the earlier work and the resulting determination of the theoretical scaling parameters have been concerned with systems of relatively high or low T_g's and with oligomers.[5,7] Second, systematically varying thermodynamic histories were used to reach the glassy state. These are particularly appropriate for analyses of the liquid–glass intersection in terms of the equilibrium theory and for establishing the behavior of the theoretical ordering parameter in the glassy state.

The experimental procedure used to obtain the PVT data is given in detail in ref 6. In all observations the maximum pressure was restricted to 800 bars. (The conversion to corresponding SI units is 1 bar = 0.1 megapascals (MPa).) Liquid data were taken over a temperature range of 35 to 100° with the lower limit established by the length of time the authors were willing to allow to attain equilibrium. Three thermodynamic histories were employed to form the glass, namely: (a) variable formation, (b) constant formation at atmospheric pressure, and (c) constant formation at 800 bars. With all histories the glass was formed by isobaric cooling at a constant rate of 5°C/hr. With the variable formation history (a) the glass was formed by repeated isobaric cooling paths, each commencing at a different pressure in the liquid state. Using the constant formation history (b) the glass was obtained by isobaric cooling at atmospheric pressure, with subsequent data taken at different pressures within the glassy region. History (c) is the same as (b) except that the glass was formed at 800 bars. With glasses (b) and (c) sufficient time was allowed at each temperature and pressure to attain thermal equilibrium, but the measurements were made fast enough for no significant viscoelastic relaxation in volume to occur. Although glasses (b) and (c) are of course not in true equilibrium, the data may be used to evaluate proper equations of state since all paths are reversible under these conditions. A principal distinction in procedure between the variable formation history (a) and the constant formation histories (b) and (c) is that with (a) all pressure changes occur in the liquid region, whereas, with (b) and (c) they are made in the glass.

The PVT surfaces evaluated from these histories are illustrated schematically in Figure 1, which shows the relationship between the liquid and the three glasses in PVT space. Note that the liquid and various glass surfaces are continuous through their respective glass transition intersection lines. In principle it is possible to obtain these surfaces experimentally through appropriate variations in temperature and pressure.[6]

The consequences of the three different histories are indeed distinct. The glass PVT surface obtained from history (a) is actually a surface constructed to contain the isobaric cooling curves of a series of glasses that have undergone their glass transitions at different temperatures and pressures. Each of the glasses therefore has different thermodynamic properties which pertain to different conditions of formation, hence the designation "variable formation." Accordingly, the surface does not represent the thermodynamic properties of a "single physical substance," or more specifically a single glass. However, the liquid–glass intersection temperature $T_g(P)$ is an important kinetic property which has been argued[6,8] to approximate the isoviscous state. This view is confirmed by the values of dT_g/dP

Table I
Volume–Temperature Coefficients and Uncertainties for the Relation $V_0 = A_0 + B_0T + C_0T^2$ At Atmospheric Pressure[a]

	$A_0 \pm \Delta A_0$	$(B_0 \pm \Delta B_0) \times 10^3$	$(C_0 \pm \Delta C_0) \times 10^6$	$\Delta V_0/V_0$, %	Temp range
Liquid	0.82485 ± 0.00011	0.5855 ±0.0035	0.282 ± 0.026	0.0040	$35 \leq T \leq 100$
Glass a and b	0.835852 ± 0.000015	0.23451 ± 0.00092		0.0058	$-30 \leq T \leq 20$
Glass c	0.830013 ± 0.000030	0.2465 ±0.0035	0.51 ± 0.15	0.0080	$-30 \leq T \leq 10$

[a] T in °C, V in cm³/g.

which are in close agreement with those obtained from dynamic mechanical and dielectric time–temperature–pressure superposition.[9,10] Histories (b) and (c) yield the proper thermodynamic properties of a "single physical substance" (hence the name "constant formation") but give very little information with respect to the relationship of kinetics to pressure. As indicated in Figure 1, history (c) for which the glass is formed at an elevated pressure produces a more densified glass than (b).

In order to distinguish between the properties of glasses formed by different histories, it is proper and convenient to consider two sets of variables.[6] When forming a glass by constant rate of cooling r under pressure P', the specific volume V is determined experimentally by the function $V(T,P,P',r)$. The first set comprises the symbols T and P which denote the temperature and pressure for each data point in any given experiment. The second set comprises P' and r which give the conditions of glass formation. Accordingly, T and P are proper state variables, whereas P' and r are parameters describing the history.

In keeping with a convention similar to that used by Goldstein,[8] $T_g^\dagger$ is the intersection line of the PVT liquid and glass surfaces. ($T_g^\dagger$ used here is identical in meaning to the T_g^* in ref 6 and 8. This change in symbols is made to preclude the possibility of confusing T_g^* with the scaling parameter T^* used here and in related papers on corresponding state theories.) In this work $T_g^\dagger = T_g^\dagger(P,P')$ (since r is the same in all instances). In the special case $P = P'$, as is always true with the variable formation history (a), $T_g^\dagger(P,P') = T_g(P)$. T_g (without the superscript †) measures a kinetic or relaxational property and is taken to be the proper glass transition temperature. $T_g^\dagger$ or $(\partial T_g^\dagger/\partial P)_{P'}$, which we take to be $dT_g^\dagger/dP$, measures a thermodynamic property defined from the proper equations of state of the equilibrium liquid and constant formation glass in a metastable state.

With glasses at sufficiently low temperatures where structural relaxation times are very long with respect to experimental times, the structure may be considered to be "frozen in" with respect to mechanical and thermodynamic disturbances. This assumption implies that a set $\{Z\}$ of ordering parameters of the glass be constant with temperature and pressure. This hypothesis will be tested on the constant formation glasses in the extension of the hole theory to the glassy state.

In evaluating experimental data the temperature and pressure are usually taken as the independent variables. This choice of independent variables is appropriate in view of the fact that the density is measured as a function of temperature and pressure and is determined uniquely for a specified thermodynamic history. Consequently, in following this procedure, there is no distinction between the reduced experimental and reduced theoretical values of temperature and pressure, but as a result of experimental error and inaccuracies in the theory, distinctions will exist between theoretical and experimental values of all other quantities. Thus, for example, there is a slight difference between the numerical magnitudes of the reduced experimental equilibrium volumes and those of the corresponding theoretical ones.

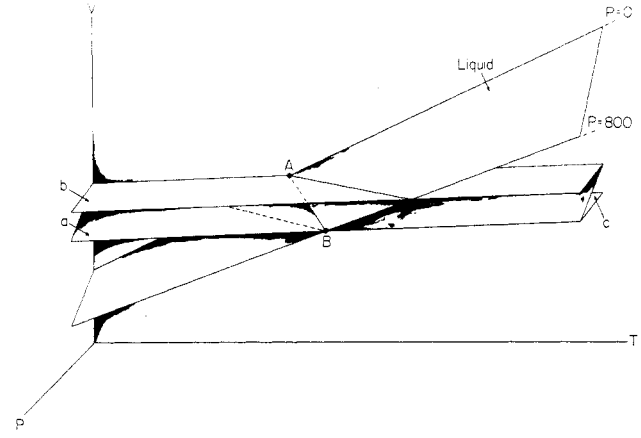

Figure 1. Schematic diagram illustrating PVT liquid and glass surfaces; (a) variable formation (b) glass formed at atmospheric pressure, and (c) glass formed at 800 bars. For explanation of points A and B see text.

Results and Discussion

1. Evaluation of Tait Parameters. As in the previous work of Simha and coworkers,[5,7] the Tait relation

$$1 - V(T,P)/V_0(T) = C \ln [1 + (P - P_0)/B(T)] \quad (1)$$

is used here to facilitate the evaluation of the PVT data for both liquid and glasses. In eq 1, V_0 represents the volume at an arbitrary reference pressure P_0, which in this work is taken as atmospheric pressure ($P_0 = 0$, gage pressure). The universal value of $C = 0.0894$, which has been applicable to all polymers investigated previously, is observed to apply here as well as to both liquid and glassy regions. Also, as in previous work, the temperature dependence of B is described by the relation[5,7]

$$B(T) = a \exp(-bT) \quad (2)$$

We have evaluated the Tait parameters by means of a slightly different procedure from that used in previous work. Since there were not always available values of V_0 corresponding to those of V at elevated pressures and the same temperature, V_0 for each experimental isotherm was determined from a quadratic fit of the form

$$V_0 = A_0 + B_0T + C_0T^2 \quad (3)$$

The OMNITAB polyfit routine[11] was employed, treating the liquid and each of the glassy regions separately. The results are tabulated in Table I, which includes the values of the above coefficients with their standard deviations, the residual volume standard deviations ($\Delta V_0/V_0$), and the ranges of data from which these quantities were determined.

Table II
Tait Parameters and Uncertainties for the Relation $B(T) = a\exp(-bT)^a$

	$a \pm \Delta a$	$(b \pm \Delta b) \times 10^3$	$\Delta V_0/V_0$, %	Range
Liquid	2035.4 ± 7.9	4.257 ± 0.052	0.015	$(30 + 0.020P) \leq T \leq 100$
Glass a	2292.3 ± 4.3	0.890 ± 0.099	0.027	$-30 \leq T \leq (20 + 0.020P)$
Glass b	3079.3 ± 8.2	0.97 ± 0.16	0.035	$-30 \leq T \leq 10$
Glass c	3143.7 ± 5.2	2.637 ± 0.091	0.035	$-30 \leq T \leq (10 + 0.040P)$
				$0 \leq P \leq 800$

[a] T in °C, P in bars.

Since the value of C is predetermined, the computation of the parameters a and b is a simple matter. Equation 2 is rewritten in linear form

$$\ln a - bT = \ln B(T) \tag{4}$$

and B_i is calculated at each experimental point i from the expression

$$B_i = P_i\{\exp[(1/C)(1 - V_i/V_0)] - 1\}^{-1}$$

The parameters a and b are then evaluated for each data set by a linear regression on eq 4, using values at every experimental T_i and P_i. The results are exhibited in Table II, which includes the parameters with their standard deviations, the residual volume standard deviation, and the approximate experimental ranges from which these quantities were determined.

In ref 6 polynomials of the form

$$V = \sum_{i=0}^{2}\sum_{j=0}^{2} a_{ij}T^iP^j \tag{5}$$

were used to fit these data. (The small differences between the values of the coefficients in eq 5 shown in Table I and the corresponding ones of ref 6 are artifacts which result from the difference between the statistical treatments. Those in Table I are more accurate, but their application is restricted to atmospheric pressure.) Although eq 5 produces a better fit to the volumes than eq 1, there is some question regarding the validity of the temperature and pressure derivatives. Anomalous behavior was observed in the internal pressure results derived from eq 5. Since these anomalies were not observed with corresponding calculations using the Tait equation, and since it has been used in previous investigations, its application will be continued for most of these analyses. The transition temperatures, however, were evaluated previously using eq 5 with appropriate coefficients. The values of these coefficients and the transition temperatures with their 95% confidence bounds are given in ref 6.

2. Evaluation of Theoretical Scaling Parameters. The theoretical PVT relation is expressed in terms of the dimensionless reduced variables

$$\tilde{P} = P/P^* \tag{6a}$$

$$\tilde{V} = V/V^* \tag{6b}$$

$$\tilde{T} = T/T^* \tag{6c}$$

Here P^*, V^*, and T^* are the characteristic scaling parameters which provide the connection between theory and experiment. Pairs of these quantities may be used to obtain the corresponding states between different polymers according to the theory. The theoretical equation of state in terms of the occupied site fraction y is[2a]

$$\tilde{P}\tilde{V}/\tilde{T} = [1 - 2^{-1/6}y(y\tilde{V})^{-1/3}]^{-1} + (2y/\tilde{T})(y\tilde{V})^{-2}[1.011(y\tilde{V})^{-2} - 1.2045] \tag{7}$$

At equilibrium the equation of constraint is

$$(s/3c)[1 + y^{-1}\ln(1 - y)] = (y/6\tilde{T})(y\tilde{V})^{-2}[2.409 - 3.033(y\tilde{V})^{-2}] + [2^{-1/6}y(y\tilde{V})^{-1/3} - 1/3][1 - 2^{-1/6}y(y\tilde{V})^{-1/3}]^{-1} \tag{8}$$

where s and $3c$ are the number of segments per chain and external degrees of freedom per chain, respectively. As in previous work, the value of s/3c = 1 will be used here. Equation 8 is the condition for the minimization of the Helmholtz free energy with respect to the ordering parameter y. Accordingly, the explicit equilibrium equation of state is obtained from a simultaneous solution of eq 7 and 8 by which y is eliminated. Since it is not possible to write this equation in closed form, numerical solutions are obtained by Newton's iteration method.

In previous work the scaling parameters V^* and T^* were determined by visual curve shifting to obtain volume–temperature superposition at atmospheric pressure. We will employ instead a numerical procedure. It has been previously shown that the combination of eq 7 and 8 at atmospheric pressure may be approximated over a large range of $\tilde{T}$ by the interpolation relation[12]

$$\ln \tilde{V} = A + B\tilde{T}^{3/2} \tag{9}$$

The values $A = -0.1034$ and $B = 23.835$ obtained from a least-square fit give a standard deviation of 0.16% over the range

$$1.65 < \tilde{T} \times 10^2 < 7.03$$

which includes the ranges of most of the polymers and oligomers investigated. In this work even higher accuracy is attained by limiting the range applicable to the current data for which $A = -0.10340$ and $B = 23.785$ with a residual standard deviation of 0.0033%. The corresponding relation was fitted to the experimental data from which the values $C = -0.3080$ and $D = 0.000026$ were obtained by linear regression. By substitution of eq 6b and 6c into eq 9 it is seen that the conditions for superposition of eq 9 and 10 are

$$\ln V = C + DT^{3/2} \tag{10}$$

$$V^* = \exp(C - A)$$
$$T^* = (B/D)^{2/3} \tag{11}$$

and thus $T^* = 9419$ K and $V^* = 0.8141$ cm³/g.

The results are shown in Figure 2 where ln $\tilde{V}$ is plotted

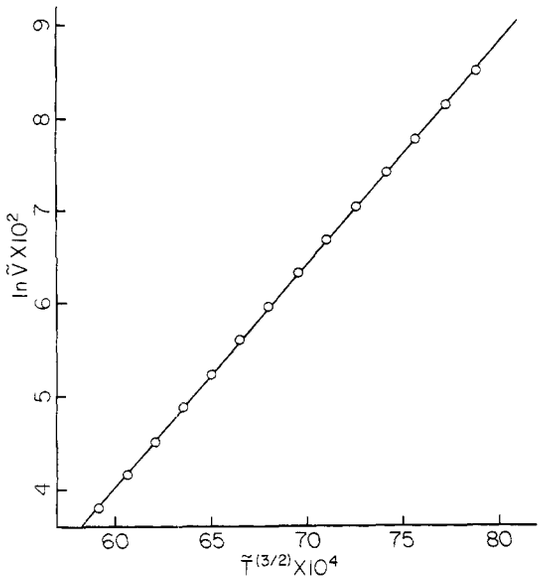

Figure 2. Reduced volume–temperature curve at atmospheric pressure: (O) experimental; (——) theory.

as a function of $\tilde{T}^{3/2}$. The solid line represents the response derived from the theory, eq 7 and 8, with $\tilde{P} = 0$, which is indistinguishable from eq 9. The circles indicate the reduced experimental values of ln (V_i/V^*). The agreement is very satisfactory, but an enlarged plot reveals a clear tendency toward larger reduced experimental values at midrange and smaller ones at the extremities than the theoretical values. This trend is tantamount to a larger temperature dependence of the theoretical than the experimental thermal expansion and is consistent with previous observations.[4]

Another test on the theory is to calculate values of T^* and V^* necessary to superpose the volume V and isobaric thermal expansivity α exactly at each data point.[4] Noting that $\alpha T = \tilde{\alpha}\tilde{T}$, it is seen that eq 9 is equivalent to

$$\ln \tilde{V} = A + \tfrac{2}{3}\alpha T \tag{12}$$

From these equations the following relations for the scaling parameters at each data point i result

$$\begin{aligned} T_i^* &= T_i/\tilde{T}_i = [3B/(2\alpha_i)]^{2/3} T_i^{1/3} \\ V_i^* &= V_i/\tilde{V}_i = V_i/\exp[A + \tfrac{2}{3}\alpha_i T_i] \end{aligned} \tag{13}$$

with α_i's computed by means of eq 3. We observe T_i^* to vary from 9149 to 9674 with increasing temperature with a standard deviation of 0.54%. Corresponding values of V_i^* vary from 0.80881 to 0.81991 with a standard deviation of 0.13%. The average values $T^* = 9416$ and $V^* = 0.8143$ are slightly different from those obtained from eq 11, where the fit is entirely to volume–temperature. With the procedure leading to eq 13 there is a compromise between volume–temperature and thermal expansion–temperature. Since visual volume–temperature superposition was used in previous work, the procedure leading to eq 11 appears to be more appropriate for comparisons with other polymers and will, accordingly, be used in this work. The sign and magnitude of the temperature variations in T^* and V^* are in accord with the results for other polymers and can be interpreted as a decrease in the effective number of external degrees of freedom and an increase in the size of the effective segment with increasing temperature.[4]

It remains to determine P^* from the data at elevated pressures. With T^* and V^* known, the P_i^* are calculated

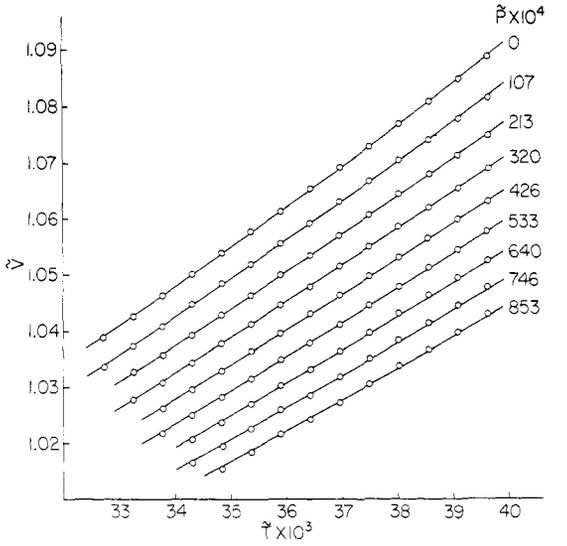

Figure 3. Isobars in reduced coordinates: (O) experimental in the liquid region; (——) theory.

Table III
Scaling Parameters and Uncertainties

	Units	Value	St dev, %	Data points
T^*	K	9419	0.54	14
V^*	cm³/g	0.8141	0.13	14
P^*	bars	9380	1.7	96

for a series of points i by means of the relation

$$P_i^* = \left(\frac{P_i V_i T^*}{V^* T_i}\right)\left(\frac{\tilde{P}\tilde{V}}{\tilde{T}}\right)_i^{-1}$$

where the term in the second set of parentheses is obtained from the theory, eq 7 and 8. An average value of $P^* = 9380$ bars results in this manner with a residual standard deviation of 1.7% over 96 values.

The scaling parameters are summarized in Table III. The deviations for T^* and V^* are those obtained from superposing the volumes and thermal expansions exactly. Figure 3 depicts the results of the superposition, where the reduced specific volume is plotted as a function of reduced temperature at a series of reduced pressures. The circles and solid lines represent experiment and theory, respectively. The temperatures range from 35 to 100° in 5° increments and the pressures from 0 to 800 bars in 100-bar increments.

Since the T^* and V^* were evaluated at atmospheric pressure, the superposition is somewhat better at atmospheric than at elevated pressure. Although an evaluation of the scaling factors from all data points would produce a better overall fit, the method used here gives values of T^* and V^* which are independent of the experimental pressure range. Note that it is only possible to evaluate P^* from the data at elevated pressures. The very satisfactory overall agreement between experimental and theoretical isobars displayed in Figure 3 is consistent with the results of previous investigations.

3. Analysis of the Liquid-Glass Transition. An appropriate test of the theory is provided by investigating the behavior of the ordering parameter, namely the hole fraction $h = 1 - y$, along the transition line $T_g(P)$, as defined by the intersection of the liquid and variable formation glass (a) surfaces in PVT space (see intersection A–B in Figure

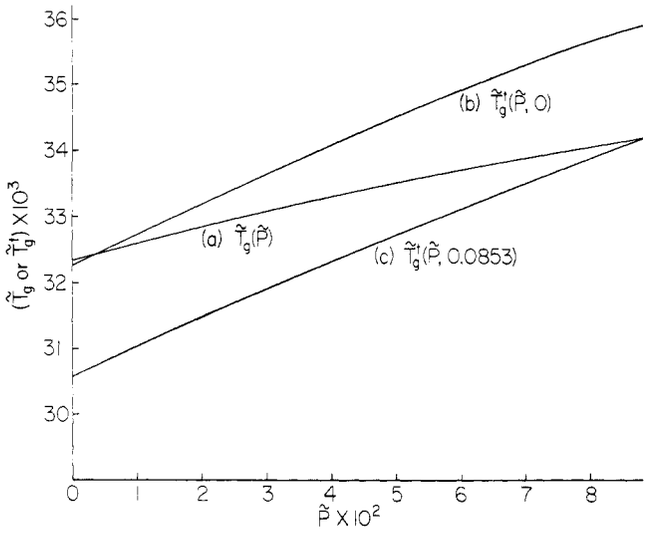

Figure 4. Transition lines (reduced glass temperature *vs.* reduced pressure) for the different thermodynamic histories: (a) variable formation, (b) constant formation at atmospheric pressure, (c) constant formation at 800 bars.

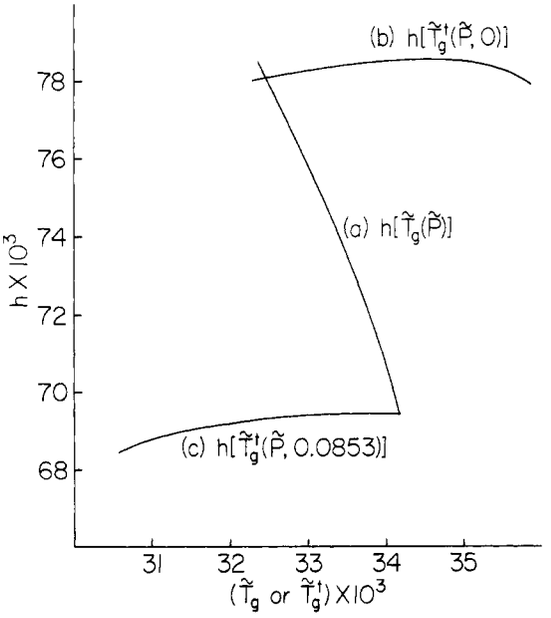

Figure 5. Variation of hole fraction h with T_g or $T_g^\dagger$, corresponding to different pressures; see Figure 4.

1). In doing this we follow the principle of analysis given previously.[13] From an equation of state of the form $f(T,P,h) = 0$ there follows at $T = T_g$

$$dT_g/dP = (\partial T/\partial P)_h + (\partial T/\partial h)_P(dh/dP) \quad (14)$$

In view of the fact that eq 14 represents a generally valid relationship, any attempted numerical evaluations as a test would be redundant. The meaningful test of the theory then consists of examining the assumed relation for a constant formation glass

$$dT_g^\dagger/dP = (\partial T/\partial P)_h \quad (15)$$

where values of the quantities on the left and right-hand sides are obtained from experiment and theory, respectively. This relation implies that the glass transition for a "single physical substance" occurs at a fixed value of h.

The relation

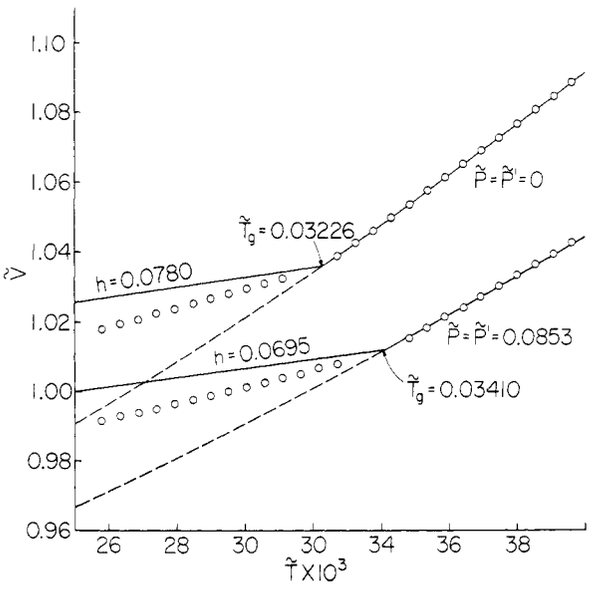

Figure 6. Reduced volume–reduced temperature plots for the two cases where $P = P'$. Continuous and dashed lines, from equilibrium equation of state. Lines commencing at T_g from equation of state, eq 7 subject to constraint condition $h = h[T_g(P')]$: (O) experimental.

$$dT_g^\dagger/dP = \Delta\kappa/\Delta\alpha \quad (16)$$

where κ is the isothermal compressibility and the Δ's indicate differences in the respective quantities between liquid and glass, holds in general. This relation is a tautological result,[6,8,14] *i.e.*, a geometrical consequence of the intersection of two surfaces in three-dimensional space.

Using eq 15 and 16 we can rewrite eq 14 as the Ehrenfest-type relation

$$dT_g/dP = \Delta\kappa/\Delta\alpha + (\partial T/\partial h)_P(dh/dP) \quad (17)$$

which may also be used to examine the predictions of the theory in a nontrivial way. Although conformity with eq 15 is tantamount to that with eq 17, perusal of both is important to obtain a more quantitative test of the theory.

In eq 17 dT_g/dP is evaluated from the variable formation history (a). $\Delta\kappa/\Delta\alpha$ is obtained from either of the constant formation histories (b) or (c) along with their respective transition lines $T_g^\dagger$. There are only two points in PVT space at which we have sufficient data to evaluate both dT_g/dP and $\Delta\kappa/\Delta\alpha$ under the same conditions. These are indicated by points A and B in Figure 1, for which $T_g = T_g^\dagger$ ($P = P'$), and is true only at 0 and 800 bars in our set of experiments. Furthermore $(\partial T/\partial h)_P$ is evaluated from the theoretical equation of state, eq 7 and 8. Similarly, dh/dP is computed from the theory along the transition line $T_g(P)$, as obtained from experiment.

We proceed to evaluate eq 15 and 17. Figure 4 is a reduced plot of the transition temperature as a function of pressure for the variable (a) and constant formation histories (b) and (c). The fact that these curves do not intersect precisely at abscissas 0 and 0.0853 (800 bars) is an artifact introduced by the statistical fit[6] of the data. The values of these functions were calculated from the identical set of PVT data in the liquid region but each from a different set in the glass. However, the sets in the glass have common subsets at either 0 or 800 bars corresponding to the intersections in Figure 4. It has been shown that values of the transition temperatures at the two intersections fall within the 95% confidence limits predicted from analysis of each set.[6] Figure 5 illustrates the hole fraction $h = 1 - y$ calcu-

lated from the theoretical liquid equation of state as a function of the reduced transition temperatures given in Figure 4. According to the assumption leading to eq 15, these curves should resemble a mirror image of the letter Z, with h being constant over the two constant formation histories, but with a different value for each. The curves approximate this form with the range of h for history (a) being about 12% compared with about 1% for either of histories (b) or (c). It is not clear whether these deviations over either of the constant formation histories (b) or (c) are significant or are artifacts resulting from the experimental uncertainty in determining the transition temperatures.

As stated earlier, we have sufficient data to evaluate eq 15 at 0 and 800 bars, which correspond to the intersection pressures shown in Figure 4. Using numerical methods, the appropriate reduced values were obtained and are given in parenthesis below the quantities to which they apply.

$$(\partial\tilde{T}/\partial\tilde{P})_h = \Delta\tilde{\kappa}/\Delta\tilde{\alpha}$$
$$(0.0453) \leftrightarrow (0.0480) \qquad \tilde{P}' = 0$$
$$(0.0376) \leftrightarrow (0.0373) \qquad \tilde{P}' = 0.0853$$

The agreement between these values is considered to be good, in particular at 800 bars. To the extent to which the above equation holds, the modified Ehrenfest relation, eq 17, should be obeyed also. The evaluation in terms of reduced variables is summarized below.

$$d\tilde{T}_g/d\tilde{P} = \Delta\tilde{\kappa}/\Delta\tilde{\alpha} + (\partial\tilde{T}/\partial h)_P(dh/d\tilde{P})$$
$$(0.0264) \leftrightarrow (0.0480) + (0.1746)(-0.1036) = (0.0299) \qquad \tilde{P}' = 0$$
$$(0.0148) \leftrightarrow (0.0373) + (0.2080)(-0.1093) = (0.0146)$$
$$\tilde{P}' = 0.0853$$

Again the agreement is good, in particular at 800 bars.

We conclude that the theoretical ordering parameter $h = 1 - y$ behaves indeed properly and this once more indicates the quantitative success of the theory in the glass transition region. The nonconstancy of h at T_g, as contrasted with $T_g^\dagger$, implies that no obvious "iso-condition" for the onset of the glass transition under different formation conditions for a given polymer can be formulated within the frame of this equilibrium theory. We have previously shown that the reduced glass temperature at atmospheric pressure and the magnitude of h at T_g for different polymers are not universal.[4]

4. The Liquid-Glass System. In the preceding section it was shown that the ordering parameter is essentially constant along the experimental transition line $T_g^\dagger(P)$, which pertains to a "single physical substance." Going still further we will test the simple assumption that this ordering parameter be constant with temperature and pressure for each of the constant formation glasses. The constancy of h along a given $T_g^\dagger$ line does, of course, not imply a corresponding behavior in the glass. On the other hand, it is obvious that constancy of h in the glass would also require constancy along $T_g^\dagger$.

Figure 6 exhibits two sets of reduced volume–temperature curves corresponding to $P = P' = 0$ and 800 bars, respectively. Since $P = P'$, these curves may be taken from either the variable or constant formation histories. The open circles give the reduced experimental values for both liquid and glass. Above $T_g(P)$ the solid curves represent the theoretical equilibrium values. Below T_g the solid curve of each set gives the theoretical value of V corresponding to the constant value of $h = 1 - y$ with $h = h[T_g(P)]$. This constraint condition replaces the equilibrium condition, eq 8. The dashed lines of each set indicate the supercooled values which would be predicted by equilibrium theory. These curves are simply extensions of the liquid equation of state to temperatures below T_g and could in principle be approximated experimentally by allowing sufficient times for the completion of all relaxation processes. The vast distinction in the glassy region between the slopes of the experimental volume–temperature curves (open circles) and those for constant h leads to the conclusion that the constraint condition $h = h(T_g)$ is an oversimplification for the glass, in accord with previous observations.[4,5,13] The very good agreement in the liquid region, based on the eqilibrium condition, eq 8, indicates the reality of this effect.

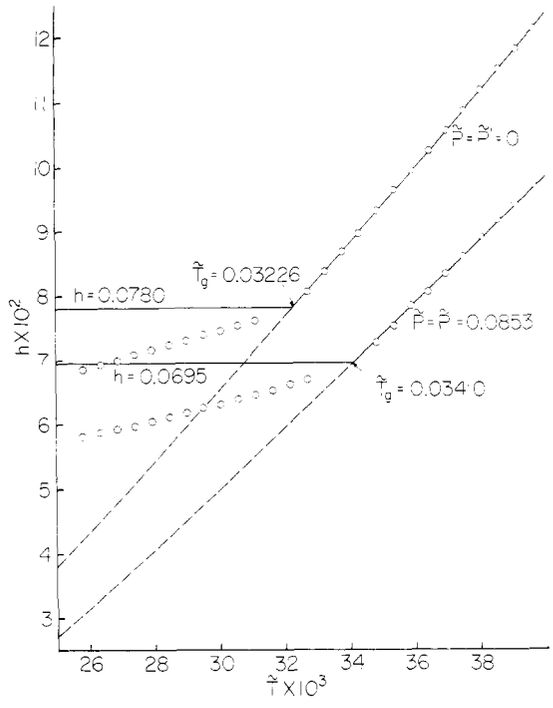

Figure 7. Hole fraction as a function of reduced temperature for the two cases where $P = P'$. Continuous and dashed lines from equilibrium equation of state. Horizontal solid lines, values of h obtained at their respective T_g's. (O), values of h obtained from equation of state, eq 7, and reduced experimental volumes.

In treating the equation of state of the glass, Quach and Simha[13] have retained eq 7 and considered h as an adjustable parameter to be obtained by experiment. The open circles in Figure 7 show the values of h derived in this manner. At temperatures above T_g the solid line again represents the equilibrium state and is continued as the dashed line in the supercooled region below T_g. The horizontal lines mark the values of h at their T_g's which are used as the oversimplified constraint condition to replace eq 8.

From inspection of Figures 6 and 7 it is clear that using the theory with one ordering parameter is not appropriate to describe the glass. The structure of the glass does not appear to be completely "frozen" as would be implied by a constant set of ordering parameters which retain their constant values at temperatures below T_g. With respect to the latter it is possible to specify quantitatively the variation of "freezing" of the glass by defining a freezing fraction as

$$F_T = 1 - \left[\left(\frac{\partial h}{\partial T}\right)_{P,\text{glass}} \Big/ \left(\frac{\partial h}{\partial T}\right)_{P,\text{liquid}}\right]$$

based on temperature,[4] or

$$F_P = 1 - \left[\left(\frac{\partial h}{\partial P}\right)_{T,\text{glass}} \Big/ \left(\frac{\partial h}{\partial P}\right)_{T,\text{liquid}}\right]$$

based on pressure. In the above equations the bounds 0 and 1 correspond to complete liquid-like behavior and complete freezing (constant h), respectively. Since h is slightly non-

Table IV
Properties of the Liquid–Glass System at $\tilde{T}_g$

	$\tilde{P} = \tilde{P}' = 0$				$\tilde{P} = \tilde{P}' = 0.0853$ (800 bars)			
	Experimental		Theoretical		Experimental		Theoretical	
	Liquid	Glass	Liquid	Glass	Liquid	Glass	Liquid	Glass
$\tilde{T}_g$	0.03226				0.03410			
$\tilde{V}$	1.0356		1.0359		1.0113		1.0119	
h	0.0777		0.0780		0.0688		0.0695	
$d\tilde{T}_g/d\tilde{P}$	0.0264				0.0148			
$\Delta\tilde{\kappa}/\Delta\tilde{\alpha}$ [a]	0.0480				0.0372			
$\tilde{\alpha}$	6.70	2.63	6.48	1.362	5.47	2.55	5.27	1.296
$\tilde{\kappa}$	0.467	0.272	0.450	0.233	0.354	0.245	0.342	0.201
$(\partial h/\partial \tilde{T})_{\tilde{P}}$	6.04	1.459	5.73	0	5.08	1.550	4.82	0
$-(\partial h/\partial \tilde{P})_{\tilde{T}}$	0.268	0.0431	0.247	0	0.191	0.0544	0.1760	0
$(\partial \tilde{T}/\partial \tilde{P})_{\tilde{V}}$	0.0697	0.1032	0.0694	0.1711	0.0648	0.0961	0.0649	0.1549
$(\partial \tilde{T}/\partial \tilde{P})_h$	0.0444	0.0296	0.0430	*b*	0.0376	0.0351	0.0365	*b*
F_T	0.758		1		0.695		1	
F_P	0.839		1		0.715		1	
F_T	0.745				0.678			
F_P	0.826				0.691			

[a] Identical with $d\tilde{T}_g\dagger/d\tilde{P}$. [b] Indeterminate.

linear with respect to temperature and pressure, the magnitudes of the F factors will not be strictly constant.

The properties of the liquid–glass system are summarized in Table IV for the two constant formation glasses evaluated at $T_g^{\dagger}(P,P') = T_g(P)$ with $P = P' = 0$ and 800 bars. In the columns labeled experimental, the values are calculated from the reduced experimental data obtained at temperatures above and below T_g, respectively. The quantities involving h are derived from eq 7 with $T = T_g$ and P taken as the independent variables and V as determined by experiment. In the theoretical columns, T_g and P are again taken as the independent variables, and the other quantities computed from eq 7, with the equilibrium constraint condition, eq 8, for the liquid and $h = h[T_g(P)]$ for the glass.

Using the above rules, most of the quantities in Table IV are self-explanatory. Since the theory does not predict T_g, there are no theoretical values for T_g and related quantities, and since the properties are evaluated at T_g, there is no distinction between the liquid and glass values of V and h. With the exception of dT_g/dP all quantities are evaluated from the constant formation histories. Note that there is only a slight distinction between the theoretical and experimental liquid values of all quantities, which indicates the good agreement with equilibrium theory as mentioned earlier. The derivative $(\partial T/\partial P)_V$ is included for comparison with the other similar derivatives tabulated. Since $(\partial T/\partial P)_h$ is expected to be equal to those for the constant formation transitions, this quantity should be independent of whether it was evaluated from either liquid or glass and should be equal to $dT_g^{\dagger}/dP = \Delta\kappa/\Delta\alpha$. The relationship $(\partial T/\partial P)_h = \Delta\kappa/\Delta\alpha$ appears to hold except for the atmospheric pressure glass ($(\partial T/\partial P)_h = 0.0296$). The discrepancy may be explained by the relatively large initial slope of the h *vs.* $T_g^{\dagger}$ curve in the atmospheric pressure glass (b) in Figure 5 and, correspondingly, the agreement with the 800-bar glass results from the relatively constant region of the right-hand region of curve c. The F factors are calculated in two meaningful ways as is indicated by the sets of values in the experimental columns and the experimental–theoretical columns. One may argue that it is more consistent to calculate the derivatives of h from eq 7 alone rather than eq 7 and 8 for the liquid and eq 7 alone for the glass (with V determined from experiment). The inclusion of the F factors using the latter procedure (last two rows) is justified since the equilibrium theory is quantitatively satisfactory. Consequently, there is very little distinction between the corresponding values. Also, since the latter was the method used in previous work for the calculation of F_T, it is continued here for appropriate comparisons. We have also included the values corresponding to the definition of the hypothetical completely frozen glass, $h = 1$. Note that the freezing fraction based on pressure is larger than that based on temperature, and both freezing fractions decrease with increasing formation pressure. The reasons for the differences between F_P and F_T at $P' = 0$ are not obvious. The decrease of both with increasing formation pressure may be explained through the increase in T_g, at which these properties were evaluated, with increasing pressure. However, if F_T for the 800-bar glass is evaluated under the same conditions ($T = T_g(0)$ and $P = 0$) as those for the atmospheric pressure glass, the value for the former is $F_T = 0.749$, which agrees with $F_T = 0.745$ obtained for the latter. Thus it would appear that increasing the formation pressure has no influence on the freezing fraction. If the freezing fraction characterizes the state of the glass, this result is consistent with the hypothesis that larger formation pressures do not produce glasses closer to the true equilibrium state, even though the densities are larger.[6]

5. Concluding Remarks. The agreement between the PVT properties predicted by the hole theory and experiment is very good for poly(vinyl acetate) in the liquid state and in conformity with the observations for other amorphous polymer solids and polymer melts.

The fact that h is not constant even in the constant formation glasses does not preclude the possibility that it be constant along any of the transition lines. Constancy has been observed along the constant formation transition line $T_g^{\dagger}$, and the modified Ehrenfest relation, eq 17, is valid. On the other hand it has been argued[6] and confirmed by experimental evidence that T_g approximates an isoviscous state. Now, since along the $T_g(P)$ line h is not constant, it does not specify viscosity, or relaxation time, even in the liquid state.

As to a theory of the glassy state, we have previously commented on possible approaches.[2b] The first would be a reformulation of the equilibrium theory in terms of more than one ordering parameter, to which the freeze-in hypothesis can be applied in a description of the glassy state. In the light of the quantitative success with the present formulation, a second avenue seemed more appropriate. This is the one used here and in previous studies, *i.e.*, the assumption of a finite temperature and pressure dependence of the hole fraction. Such a dependence has so far only been deduced from experiment, by treating h as an adjustable parameter. It remains to be seen whether it can be derived on theoretical grounds by taking into account the size distribution, *i.e.*, the clustering of holes with a partial maintenance of the equilibrium restraint, eq 8, for large holes,[2] and further partial freeze-in processes characteristic of subglass relaxations.[4] The whole process would then be practically completed at temperatures of the order of 50–70 K, when the assumption y = const ($\simeq 1$) results in a quantitatively satisfactory equation of state.[15] The diminution of h to very small values at these cryogenic temperatures stipulates a corresponding diminution of configurational entropy. A somewhat similar result is obtained from the theory of Gibbs and DiMarzio[16] for which the configurational entropy vanishes at a much higher temperature located approximately at $T_g - 50$.

The view has often been expressed in the literature that the glassy state, even at temperatures approaching the neighborhood of T_g, may be characterized by a complete "freeze-in" of structure. In our frame of reference, the structure is described by the parameter h (or alternatively F_T and F_P) which is a function of T and P. The detailed quantitative results obtained are therefore characteristic of the specific theoretical formulation. However, the conclusion regarding a temperature and pressure dependent structure appears to have general validity. This dependence is indicated by the existence of subglass relaxations which are clearly seen in, for example, the extensive dilatometric studies of Simha and colleagues.[17] The appearance of further discontinuities in the derivatives of h analogous to those shown in Figure 7[4,18] is, of course, an immediate consequence. In short, it appears that the general concept of the competely frozen glass, at least at higher temperatures, should be abandoned.

Along with the increase in density with increasing formation pressure there is a corresponding decrease in the hole fraction, which means that there is a corresponding decrease in the configurational volume as defined from theory. On the other hand no change was observed in the freezing fraction F_T between the 1-atm glass and 800-bar glass at the same temperature and pressure. Since the relation

$$dT_g/dP = TV\Delta\alpha/\Delta C_P \qquad (18)$$

seems to hold,[8,10] which implies a single entropy surface with respect to formation pressure, the apparent invariance of F_T with formation pressure is consistent with the hypothesis of a single entropy surface.[8] It would be interesting to examine if F_T remains constant during isothermal volume relaxation. In this connection, it is noteworthy that Bree, *et al.*,[19] have observed no significant changes in certain mechanical properties with formation pressure at the same temperature and pressure. This is in contrast to the pronounced changes in such properties during relaxation over the same volume range. Since these results suggest a correlation with entropy (being independent with formation pressure, according to eq 18), they give further incentive to the calculation of the entropy and other thermodynamic functions available from the theory. This study is presently being undertaken.

Acknowledgment. We thank the National Science Foundation for partial support of this work under Grant GH-36124 to Case Western Reserve University.

References and Notes

(1) (a) Institute for Materials Research; (b) Case Western Reserve University.
(2) (a) R. Simha and T. Somcynsky, *Macromolecules*, **2**, 342 (1969). (b) T. Somcynsky and R. Simha, *J. Appl. Phys.*, **42**, 4545 (1971).
(3) P. S. Wilson and R. Simha, *Macromolecules*, **6**, 902 (1973).
(4) R. Simha and P. S. Wilson, *Macromolecules*, **6**, 908 (1973).
(5) O. Olabisi, Ph.D. Thesis, Case Western Reserve University, August 1973. References 3–5 give references to earlier work.
(6) J. E. McKinney and M. Goldstein, *J. Res. Nat. Bur. Stands., Sect. A*, **78**, 331 (1974).
(7) A. Quach and R. Simha, *J. Appl. Phys.*, **42**, 4592 (1971).
(8) M. Goldstein, *J. Phys. Chem.*, **77**, 667 (1973).
(9) J. E. McKinney and H. V. Belcher, *J. Res. Nat. Bur. Stand., Sect. A*, **67**, 43 (1963).
(10) J. M. O'Reilly, *J. Polym. Sci.*, **57**, 429 (1962).
(11) D. Hogben, S. T. Peavy, and R. N. Varner, *Nat. Bur. Stand. (U. S.) Tech. Note*, **No. 552** (1971).
(12) R. Simha, P. S. Wilson, and O. Olabisi, *Kolloid-Z. Z. Polym.*, **251**, 402 (1973).
(13) A. Quach and R. Simha, *J. Phys. Chem.*, **76**, 416 (1972).
(14) E. Passaglia and G. M. Martin, *J. Res. Nat. Bur. Stand., Sect. A*, **68**, 273 (1964).
(15) R. Simha, J. M. Roe, and V. S. Nanda, *J. Appl. Phys.*, **43**, 4312 (1972).
(16) J. H. Gibbs and E. A. DiMarzio, *J. Chem. Phys.*, **28**, 373 (1958).
(17) See for example, J. M. Roe and R. Simba, *Int. J. Polym. Mater.*, in press, where references to earlier work are given.
(18) A. Quach, P. S. Wilson, and R. Simha, *J. Macromol. Sci., Phys.*, **B9** (3), 533 (1974).
(19) H. W. Bree, J. Hiejboer, L. C. E. Struik, and A. G. M. Tak, *J. Polym. Sci., Polym. Phys. Ed.*, **12**, 1857 (1974).